NEW MATERIALS OF B_2O_3–Bi_2O_3–Me_2O_3 (Me = Yb, Lu) SYSTEMS

M.M. Asadov and N.A. Akhmedova

Institute of Chemical Problems, National Academy of Sciences of Azerbaijan,
29, G. Javid ave., AZ 1143, Baku, Azerbaijan
E-mail: mirasadov@gmail.com
(Received 13 September 2010)

Abstract

It is shown that the Yb_2O_3–Bi_2O_3–B_2O_3 system gives a new $Yb_3Bi_2B_5O_{15}$ compound of a hexagonal crystallographic system. Based on the data on the nature of specimens and by means of X-ray study of obtained samples, we determined the boundaries of glass-formation regions in the Yb_2O_3–Bi_2O_3–B_2O_3 system. Homogeneous glasses were obtained in the following cuts: $Bi_2O_3 \cdot B_2O_3$ – Lu_2O_3–B_2O_3 up to 15 mol % Lu_2O_3; $Lu_2O_3 \cdot B_2O_3$–Bi_2O_3 up to 10 mol % Lu_2O_3; $Bi_2O_3 \cdot B_2O_3$ – $Lu_2O_3 \cdot Bi_2O_3$ up to 15 mol % Lu_2O_3. Eutectic coordinates of $LnBO_3$–B_2O_3 (Ln = Ce, Pr, Pm, Sm, Tb, Er) systems were calculated at first.

1. Introduction

Multicomponent oxide materials play an important role for finding and creating new functional inorganic materials. Materials based on complex oxides of rare earth metals have a variety of physical and physicochemical properties. These materials can be used as optical materials, oxygen sensors, ionic conductors, catalysts, etc. A wide range of transparency of borates (200–3500 nm) allows you to use these materials in the UV spectral region. In these materials, acentric structural units based on polyborate anions are present. This enhances their nonlinear optical properties. In addition Bi_2O_3-based materials have high values of the refractive index, a broad region of transparency in the visible and infrared ranges [1-13].

Phase relationships of the boundary sections of Yb_2O_3–Bi_2O_3–B_2O_3 have been previously investigated. Phase equilibria in the Bi_2O_3–B_2O_3 system were studied in [2, 3, 9]. In the Bi_2O_3–B_2O_3 system, in a stable equilibrium, five compounds are found: $Bi_{24}B_2O_{39}$ (melts incongruently at 905 K), $Bi_4B_2O_9$, $Bi_3B_5O_{12}$, BiB_3O_6 (melt congruently at 948, 995, 981, and 988 K) and $Bi_{12}B_8O_{15}$. Connection $Bi_{12}B_8O_{15}$ experiences a polymorphic transformation at 969 K. Overheated melt during cooling leads to crystallization of metastable phases $BiBO_3$ and $Bi_5B_3O_{12}$.

The Yb_2O_3–B_2O_3 system is characterized by the formation of compounds $YbBO_3$ and Yb_3BO_6. The first melts congruently at 1863 K, and the second melts incongruently [10].

Two intermediate compounds $YbBiO_3$ [12] and $Yb_7Bi_{17}O_{36}$ (x = 0.292) [13] are formed in the Yb_2O_3–Bi_2O_3 system. Binary system components are used, inter alia, to change the properties of ceramics. The process of doping of ceramics $BaTiO_3$ with components Bi_2O_3 and Yb_2O_3 leads to an increase in the Curie temperature [14].

In this work, we studied the properties in the Yb_2O_3–Bi_2O_3–B_2O_3, Lu_2O_3–B_2O_3–Bi_2O_3 and $LnBO_3$–B_2O_3 systems.

2. Experimental

Studies of phase equilibria in the Me_2O_3–Bi_2O_3–B_2O_3 system were carried out using XRD (DRON-2 diffractometer, Cu K_α-radiation, Ni-filter) and DTA (MOM derivatograph) by known methods. Me_2O_3 (Me – Yb, Lu) (high purity), Bi_2O_3 (high purity) and HBO_3 (high purity) were used as initial components. The interaction of components was studied on various sections. Synthesis of the samples was carried out in platinum crucibles in a muffle furnace. The duration of synthesis was 15 days.

3. Results and discussion

The direction of probable reactions between components of the Yb_2O_3–Bi_2O_3–B_2O_3 system was evaluated by thermodynamic method. Values of Gibbs energy $\Delta_f G_T^0$ of ternary systems were calculated for the solid state. Thermodynamic data of binary oxides were taken from references [15, 16]. Gibbs energy and enthalpy of formation of ternary compounds were calculated from the data for binary compounds using the equations [17]

$$\Delta V^0_{T,(1-x)A\cdot xB} = (1-x)\Delta V^0_{T,A} + x\Delta V^0_{T,B} + 2x\Delta V^0_{T,m} \quad (x \le 0.5) \tag{1}$$

$$\Delta V^0_{T,(1-x)A\cdot xB} = (1-x)\Delta V^0_{T,A} + x\Delta V^0_{T,B} + 2(1-x)\Delta V^0_{T,m} \quad (x \ge 0.5) \tag{2}$$

$$\Delta V^0_{T,(1-x)A\cdot xB} = (1-x)\Delta V^0_{T,A} + x\Delta V^0_{T,B} + \Delta V^0_{T,m} \quad \frac{x(1-x)}{0.25} \tag{3}$$

where $\Delta V^0_{T,m}$ are values of Gibbs energy $\Delta_f G_T^0$ and the enthalpy of formation $\Delta_f H_T^0$ of compounds of oxides with the composition x = 0.5. Values of $\Delta_f G_{298}^0$ and $\Delta_f H_{298}^0$ for the ternary Yb_2O_3–Bi_2O_3–B_2O_3 calculated from equations (1)–(3) are given in Table. 1.

Table 1. The calculated values of Gibbs energy and enthalpy of formation of ternary oxide compounds of the Yb_2O_3–Bi_2O_3–B_2O_3 system.

Compound	T_f (K)	$-\Delta_f H_{298}^0$ (kJ/mol)	$-\Delta_f G_{298}^0$ (kJ/mol)
$Bi_4B_2O_9$	948	1431	1309
$BiBO_3$	958	1832	1692
$Bi_3B_5O_{12}$	995	1682	1562
BiB_3O_6	981	1543	1443
$YbBO_3$	1863	3067	2921
Yb_3BO_6		2442	2325

The direction of probable reactions was estimated from tabular data. For example, for the reaction

$$2Bi_2O_3 + \alpha\text{-}YbBO_3 = Bi_4B_2O_9 + Yb_2O_3. \tag{4}$$

The value of $\Delta_r G_{298}^0$ in the forward direction is negative: –582 kJ / mol. Evaluation indicates that the change in a temperature range of 298–600 K have a weak effect on the value of $\Delta_r G_T^0$. To move from $\Delta_r G_{298}^0$ to $\Delta_r G_T^0$, we used the Kirchhoff equation and value of the specific heat of the components [15]. These thermodynamic evaluations of the probability of a reaction between the corresponding components in the system Yb_2O_3–Bi_2O_3–B_2O_3 are confirmed with the data of physicochemical analysis.

The properties of promising compounds $BiBO_3$ are given in [18-24]. The melting point of $BiBO_3$ compound is 955±5 K. $YbBO_3$ has a polymorphic transformation at 850 and 1314 K according to [9]. The melting temperature of $YbBO_3$ is 1863 K.

In order to obtain reliable data, the synthesized phases $BiBO_3$ and $YbBO_3$ were annealed at 600–625 K for 7 days. The alloys were prepared of these components for physical and chemical analyses.

The phase diagram of the $BiBO_3$–$YbBO_3$ system constructed by us is shown in Fig. 1.

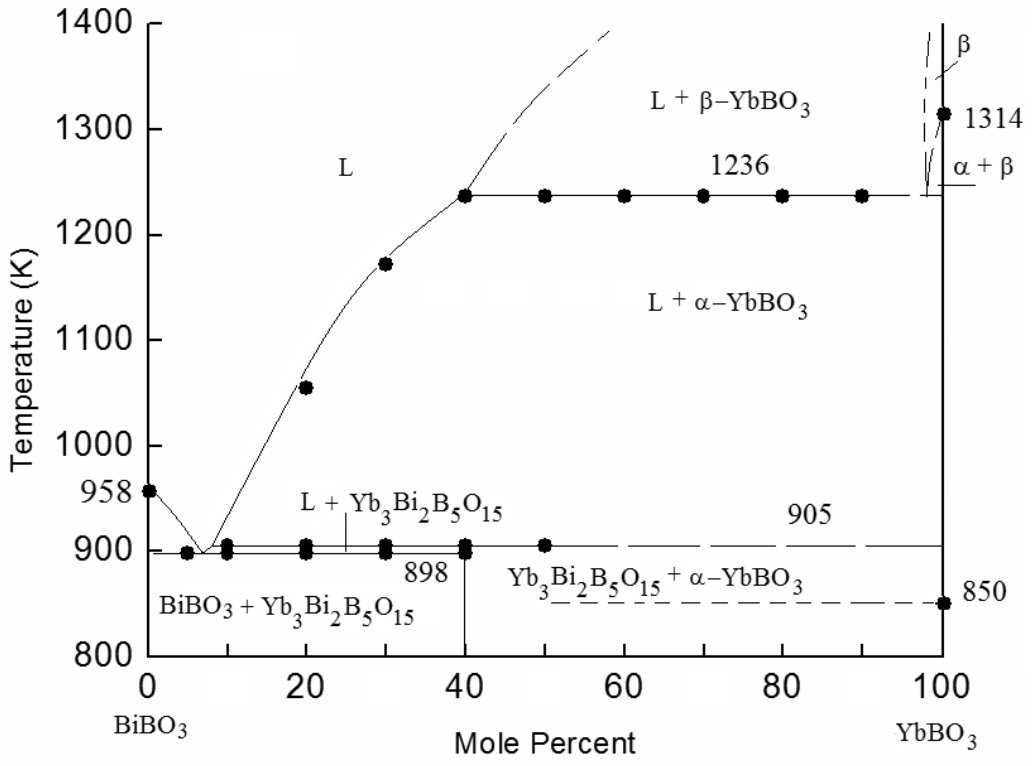

Fig. 1. Phase diagram of the $BiBO_3$–$YbBO_3$ system.

The figure shows that, in the Yb_2O_3–Bi_2O_3–B_2O_3 system, intermediate phase $Yb_3Bi_2B_5O_{15}$ is formed. This compound melts incongruently at 908 K. According to XRD patterns, the samples whose compositions correspond to $Yb_3Bi_2B_5O_{15}$ have a hexagonal system and the following cell parameters: a = 4.913 (1), c = 16.214 (1) Å.

The isothermal section of Yb_2O_3–Bi_2O_3–B_2O_3 system at 298 K was constructed as shown in Fig. 2. For this, the data on the boundary systems and data on the phase composition of synthesized samples were used. Isothermal section of the system at 298 K may be represented by 13 triangles of coexisting phases: α-$Bi_{12}B_8O_{15}$–B_2O_3–α-$YbBO_3$, α-$Bi_{12}B_8O_{15}$–BiB_3O_6–$YbBO_3$, $Bi_3B_5O_{12}$– BiB_3O_6–α-$YbBO_3$, $Bi_3B_5O_{12}$–$Yb_3Bi_2B_5O_{15}$–α-$YbBO_3$, $Bi_3B_5O_{12}$–$Yb_3Bi_2B_5O_{15}$–$BiBO_3$, $Bi_4B_2O_9$–$Yb_3Bi_2B_5O_{15}$–$BiBO_3$, $Bi_4B_2O_9$–$Yb_3Bi_2B_5O_{15}$–α-$YbBO_3$, $Bi_4B_2O_9$–Yb_3BO_6–α-$YbBO_3$, $Bi_4B_2O_9$–Yb_3BO_6–Yb_2O_3, $Bi_4B_2O_9$–α-$YbBiO_3$–Yb_2O_3, $Bi_4B_2O_9$–α-$YbBiO_3$–$Yb_7Bi_{17}O_{36}$, $Bi_4B_2O_9$–$Bi_{24}B_2O_{39}$–$Yb_7Bi_{17}O_{36}$, and Bi_2O_3–$Bi_{24}B_2O_{39}$–$Yb_7Bi_{17}O_{36}$.

Experimental data on the phase composition of synthesized samples allowed constructing the liquids surface projection of the $BiBO_3$–B_2O_3–$YbBO_3$ system. The temperatures of invariant reactions in this system are given in Table 2.

On the basis of these data about the character of specimens and by means of roentgenstudy of obtained samples, we determined the boundaries of glass-formation regions in Yb_2O_3–Bi_2O_3–B_2O_3 system. In the Yb_2O_3–Bi_2O_3–B_2O_3 system, the glass-formation region is tapered in the $Bi_2O_3 \cdot B_2O_3$–$Yb_2O_3 \cdot B_2O_3$ cut, but in $2Bi_2O_3 \cdot B_2O_3$–$Yb_2O_3 \cdot B_2O_3$ cut at composi-

tions from 10 mol % Bi_2O_3 to 40 mol % Bi_2O_3 the glasses with decreased thermal characteristics were revealed (T_{melt} = 653 K; T_{cr} = 713 K).

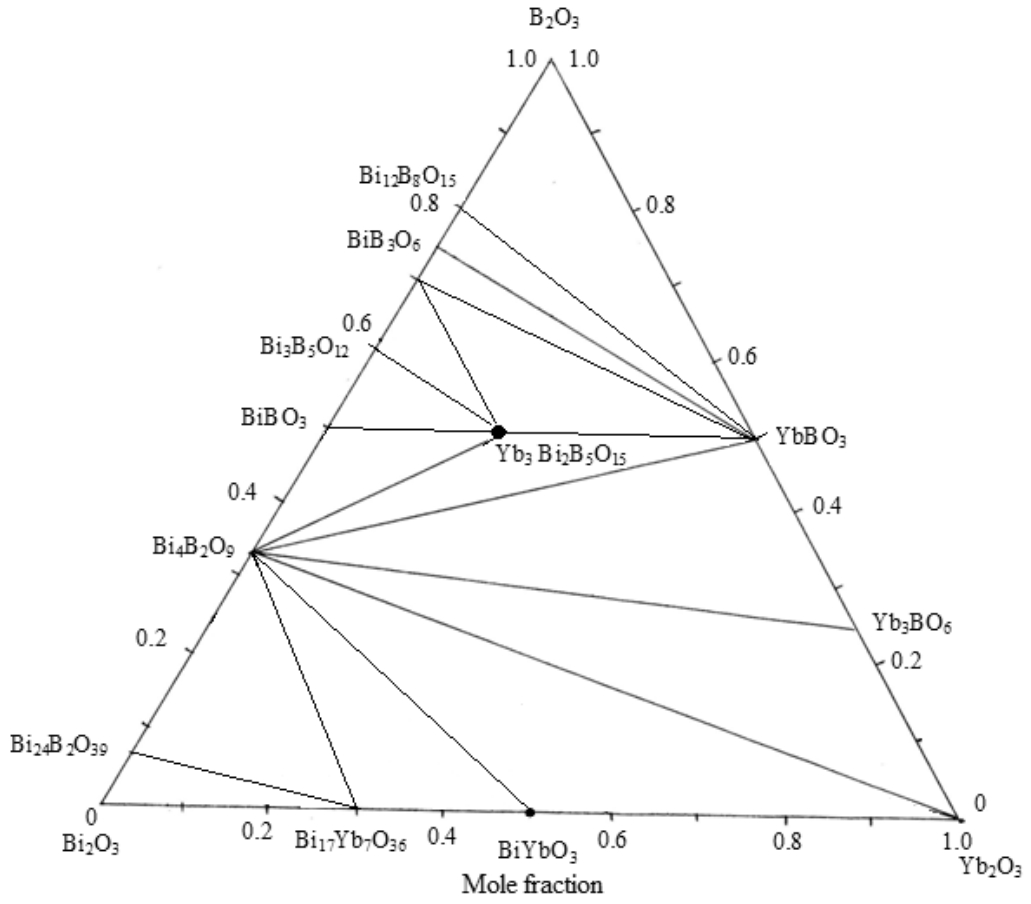

Fig. 2. Isothermal section of the Yb_2O_3–Bi_2O_3–B_2O_3 system at 298 K.

Table 2. The temperature of invariant reactions in the $BiBO_3$–B_2O_3–$YbBO_3$ system.

Reaction	Reaction type	T, K
$L \leftrightarrow BiYbO_3 + Bi_3B_5O_{12} + Yb_3Bi_2B_5O_{15}$	Eutectic (E_1)	948
$L \leftrightarrow Bi_3B_5O_{12} + \beta\text{-}YbBO_3 + BiB_3O_6$	Eutectic (E_2)	973
$L + \beta\text{-}YbBO_3 \leftrightarrow Yb_3Bi_2B_5O_{15} + Bi_3B_5O_{12}$	Peritectic (P_1)	1088
$L + \beta\text{-}YbBO_3 \leftrightarrow BiB_3O_6 + \beta\text{-}Bi_{12}B_8O_{15}$	Peritectic (P_2)	1000

The synthesis of $Bi_2O_3{\cdot}B_2O_3$ – $Lu_2O_3{\cdot}B_2O_3$, $Lu_2O_3{\cdot}B_2O_3$ – Bi_2O_3, $Lu_2O_3{\cdot}B_2O_3$ – $Lu_2O_3{\cdot}Bi_2O_3$, $Bi_2O_3{\cdot}B_2O_3$ – $Lu_2O_3{\cdot}Bi_2O_3$ systems was carried out by the solid-state-phase method. The color of specimens was varied from violent yellow to brown. In the Lu_2O_3 – B_2O_3 – Bi_2O_3 system, three regions were revealed: homogenous glasses, crystal compounds and unmixed phases. The boundaries of regions of glass-formation were determined by visually and from X-ray study of obtained specimens. Homogeneous glasses were obtained in the following cuts: $Bi_2O_3{\cdot}B_2O_3$–$Lu_2O_3{\cdot}B_2O_3$ up to 15 mol % Lu_2O_3; $Lu_2O_3{\cdot}B_2O_3$–Bi_2O_3 up to 10 mol % Lu_2O_3; and $Bi_2O_3{\cdot}B_2O_3$ – $Lu_2O_3{\cdot}Bi_2O_3$ up to 15 mol % Lu_2O_3.

In systems Ln_2O_3–Bi_2O_3–B_2O_3 based on "light" lanthanide (Ln = La–Tb) three compounds are crystallized: metaborate LnB_3O_6, orthoborate $LnBO_3$, and oxoborate

Ln_3BO_6 [11-13]. In systems Ln_2O_3–Bi_2O_3–B_2O_3 based on "heavy" lanthanides (Ln = Dy–Lu) only ortho-and oxoborates are crystallized.

Orthoborates are crystallized in different structural types of $CaCO_3$ depending on the ionic radii. The types of aragonite (La–Nd), vaterite (Sm–Yb, Y), and calcite (Lu and Sc) are stable. Boron atoms are located in isolated BO_3-triangles. The location of the structural units of BO_3-on Ln atom is different for different structural types. High refractive index (1.729–1.755), relatively low boiling temperatures of lanthanum borate glasses as compared with silicate glasses, and transparency in the a of 350–1700 nm make these glasses a promising material for photonics [11].

Correlation equations for calculation of eutectic coordinates in $LnBO_3$–B_2O_3 (Ln = La, Ce, Pr, Nd, Pm, Sm, Eu, Gd, Tb, Dy, Ho, Er, Tm, Yb, Lu) systems were proposed. Eutectic coordinates of $LnBO_3$–B_2O_3 (Ln = Ce, Pr, Pm, Sm, Tb, Er) systems were calculated at first (Table 3).

Table 3. Calculated coordinates of eutectic in systems $LnBO_3$–B_2O_3.

System	C_e, mol % B_2O_3	T_e, °C	T_{fus}, °C ($LnBO_3$)	System	C_e, mol % B_2O_3	T_e, °C	T_{fus}, °C ($LnBO_3$)
$LaBO_3$–B_2O_3	22	1136	1660	$GdBO_3$–B_2O_3	27	1232	1590
$CeBO_3$–B_2O_3	22	1140	1650	$TbBO_3$–B_2O_3	28	1280	1525
$PrBO_3$–B_2O_3	23	1144	1630	$DyBO_3$–B_2O_3	29	1328	1585
$NdBO_3$–B_2O_3	24	1148	1610	$HoBO_3$–B_2O_3	30	1368	1605
$PmBO_3$–B_2O_3	25	1150	1590	$ErBO_3$–B_2O_3	30	1396	1630
$SmBO_3$–B_2O_3	27	1157	1570	$TmBO_3$–B_2O_3	31	1424	1650
$EuBO_3$–B_2O_3	27	1172	1540	$YbBO_3$–B_2O_3	31	1446	1590
				$LuBO_3$–B_2O_3	32	1473	1650

4. Conclusions

Thus, the isothermal section of phase diagram of Yb_2O_3–Bi_2O_3–B_2O_3 at 298 K, as well as the projection of the liquid surface of $BiBO_3$–B_2O_3–$YbBO_3$, was firstly constructed. The phase diagram of the polythermal section of $BiBO_3$–$YbBO_3$ is given. The formation of $Yb_3Bi_2B_5O_{15}$ compounds with a hexagonal system and the following cell parameters: a = 4.913, c = 16.214 Å was confirmed. The obtained data can be useful for the preparation of materials with specific composition, structure and properties. On the basis of these data about the character of specimens and by means of X-ray study of obtained samples, we determined the boundaries of glass-formation regions in the Yb_2O_3–Bi_2O_3–B_2O_3 system. In the Yb_2O_3–Bi_2O_3–B_2O_3 system, the glass-formation region is tapered in the $Bi_2O_3{\cdot}B_2O_3$–$Yb_2O_3{\cdot}B_2O_3$ cut, but in 2 $Bi_2O_3{\cdot}B_2O_3$–$Yb_2O_3{\cdot}B_2O_3$ cut for compositions of 10 mol % Bi_2O_3 to 40 mol % Bi_2O_3, the glasses with decreased thermal characteristics were revealed (T_{melt} = 653 K; T_{cr} = 713 K). Correlation equations for calculation of eutectic coordinates in $LnBO_3$–B_2O_3 (Ln = La, Ce, Pr, Nd, Pm, Sm, Eu, Gd, Tb, Dy, Ho, Er, Tm, Yb, Lu) systems were proposed. Eutectic coordinates of $LnBO_3$–B_2O_3 (Ln = Ce, Pr, Pm, Sm, Tb, Er) systems were calculated at first.

References

[1] A.V. Egorysheva and Yu.F. Kargin, Neorg. Mater., 34, 859, (1998).
[2] A.V. Egorysheva, V.M. Skorikov, V.D. Volodin, O.E. Mislitskiy, and Yu.F. Kargin, Zh. Neorg. Khim., 51, 2078, (2006).
[3] A.V. Egorysheva, V.D. Volodin, and Yu.F. Kargin, Neorg. Mater., 44, 76, (2008).

[4] Yu.F. Kargin, S.N. Ivicheva, M.G. Komova, and V.A. Krutko, Zh. Neorg. Khim., 53, 474, (2008).
[5] Yu.F. Kargin, S.N. Ivicheva, and L.I. Shvorneva, Zh. Neorg. Khim., 53, 1391, (2008).
[6] A.V. Egorysheva, V.D. Volodin, and V.M. Skorikov, Neorg. Mater., 44, 1397, (2008).
[7] Yu.F. Kargin, S.N. Ivicheva, L.I. Shvorneva, M.G. Komova, and V.A. Krutko, Zh. Neorg. Khim., 53, 1614, (2008).
[8] A.V. Egorysheva, V.D. Volodin, V.M. Skorikov, and G.Y. Yurkov, Neorg. Mater., 46, 495, (2010).
[9] E.M. Levin and C.L. McDaniel, J. Am. Ceram. Soc., 45, 355, (1962).
[10] M.I. Zargarova, N.A. Akhmedova, E.S. Kuluzade, and N.M. Mustafaev, Zh. Neorg. Khim., 40, 1389, (1995).
[11] L.N. Dmitruk, O.B. Petrova, A.V. Popov, and V.E. Shukshin, Tr. IOFAN, 64, 49, (2008).
[12] The Landolt-Bornstein Database. Numerical date and Functional relationships in science and technology. Group III. Crystal structure date of inorganic compounds. Springer-Verlag. Berlin, Heidelberg, New York, London, Paris, Tokyo, 7, 121, (1987).
[13] M. Drache, P. Roussel, J.P. Wignacourt, and P. Conflant, Mat. Res. Bull., 39, 1393, (2004).
[14] G. Yao, X. Wang, Y. Yang, and L. Li, J. Am. Ceram. Soc., 93, 6, 1697, (2010).
[15] V.P. Glushko, ed. by, Termicheskie konstanty veschestv. Spravochnik v 10 vypuskah, [in Russian], Moscow, VINITI AN SSSR, 8, 1, 535, (1978).
[16] O. Kubaschewski, C.B. Alcook, Metallurgical Thermochemistry, Pergamon Press, Oxford, N.Y., Toronto, Sydney, Paris, Frankfurt, 391, 1979.
[17] V.T. Maltsev and S.A. Kutolin, Zh. Neorg. Khim., 24, 12, (1979).
[18] P. Becker, Cryst. Res. Technol., 38, 74, (2003).
[19] R. Ihara, T. Honma, Y. Benino, T. Fujiwara, and T. Komatsu, Opt. Mater., 27, 403, (2004).
[20] A.V. Egorysheva, V.I. Burkov, Yu.F. Kargin, V.G. Plotnichenko, and V.V. Koltashev, Kristallografiya, 50, 135, (2005).
[21] A. Bajaj and A. Khanna, J. Phys.: Condens. Matter., 21, 035112, (2009).
[22] P. Becker and R. Frohlich, Z. Naturforsch. B., 59, 256, (2004).
[23] Yu.F. Kargin, V.P. Zhereb, and A.V. Egorysheva, Zh. Neorg. Khim., 47, 992, (2002).
[24] H. Huppertz, J. Chem. Sci., 56b, 697, (2001).